Gready, J. E. (1985) *Biochemistry 24*, 4761-4766.
Hanahan, D. (1983) *J. Biol. Chem. 166*, 557-580.
Howell, E. E., Villafranca, J. E., Warren, M. S., Oatley, S. J., & Kraut, J. (1986) *Science (Washington, D.C.) 231*, 1123-1128.
Johnson, K. A. (1986) *Methods Enzymol. 134*, 677-705.
Kramer, W., & Fritz, H.-J. (1987) *Methods Enzymol. 154*, 350-367.
Kroeker, W. D., Kowalski, D., & Laskowski, M., Sr. (1976) *Biochemistry 15*, 4463-4467.
Legerski, R. J., & Robberson, D. L. (1985) *J. Mol. Biol. 181*, 297-312.
Mathews, C. K., & Huennekens, F. M. (1960) *J. Biol. Chem. 238*, 3436-3442.
Mayer, R. J., Chen, J.-T., Taira, K., Fierke, C. A., & Benkovic, S. J. (1986) *Proc. Natl. Acad. Sci. U.S.A. 83*, 7718-7720.
Morrison, J. F., & Stone, S. R. (1988) *Biochemistry 27*, 5499-5506.
Murphy, D. J., & Benkovic, S. J. (1989) *Biochemistry 28*, 3025-3031.
Penner, M. H., & Frieden, C. (1985) *J. Biol. Chem. 260*, 5366-5369.
Presta, L. G., & Rose, G. D. (1988) *Science (Washington, D.C.) 240*, 1632-1641.
Richardson, J. S., & Richardson, D. C. (1988) *Science (Washington, D.C.) 240*, 1648-1652.
Sanger, F. (1981) *Science (Washington, D.C.) 214*, 1205-1210.
Seeger, D. R., Cosulich, D. B., Smith, J. M., & Hultquist, M. E. (1949) *J. Am. Chem. Soc. 71*, 1753-1758.
Stone, S. R., & Morrison, J. F. (1982) *Biochemistry 21*, 3757-3765.
Stone, S. R., & Morrison, J. F. (1983) *Biochim. Biophys. Acta 745*, 247-258.
Stone, S. R., & Morrison, J. F. (1984) *Biochemistry 23*, 2753-2758.
Taira, K., & Benkovic, S. J. (1988) *J. Med. Chem. 31*, 129-137.
Taira, K., Fierke, C. A., Chen, J.-T., Johnson, K. A., & Benkovic, S. J. (1987) *Trends Biochem. Sci. (Pers. Ed.) 12*, 275-278.
Villafranca, J. E., Howell, E. E., Voet, D. H., Strobel, M. S., Ogden, R. C., Abelson, J. N., & Kraut, J. (1983) *Science (Washington, D.C.) 222*, 782-788.
Viola, R. E., Cook, P. F., & Cleland, W. W. (1979) *Anal. Biochem. 96*, 334-340.
Volz, K. W., Matthews, D. A., Alden, R. A., Freer, S. T., Corwin, H., Kaufman, B. T., & Kraut, J. (1982) *J. Biol. Chem. 257*, 2528-2536.
Williams, J. W., Morrison, J. F., & Duggleby, R. G. (1979) *Biochemistry 18*, 2567-2573.
Winberg, G., & Hammarskjold, M.-L. (1980) *Nucleic Acids Res. 8*, 253-264.

Designing an Allosterically Locked Phosphofructokinase†

Craig E. Kundrot‡,§ and Philip R. Evans*,‡

Laboratory of Molecular Biology, Medical Research Council, Hills Road, Cambridge CB2 2QH, U.K., and Department of Chemistry and Biochemistry, University of Colorado, Boulder, Colorado 80309-0215

Received July 31, 1990; Revised Manuscript Received October 23, 1990

ABSTRACT: Six site-directed mutants of *Escherichia coli* phosphofructokinase (PFK) were made in an attempt to produce an enzyme "locked" in the inactive or "T"-state. The kinetic properties of the mutants were examined as a function of the substrates fructose 6-phosphate (Fru6P) and ATP, the positive effector GDP, and the negative effector phosphoenolpyruvate (PEP). All mutants exhibited lower activity than wild-type PFK. Three mutants (RS63, LV153, and VT246) had apparent dissociation constants for substrates and effectors similar to those of wild type. One mutant, HN160, had a 10-fold reduced affinity for Fru6P and reduced apparent affinity for the effectors. Two mutants, SN159 and T(GS)156, exhibited hyperbolic kinetics consistent with a "locked" T-state protein. Surprisingly, T(GS)156 showed hyperbolic activation in response to the physiological inhibitor PEP. The mutant PFK properties are discussed in terms of the PFK structure. These results suggest that the kinetic properties of PFK are sensitive to interactions in the homotropic interface; residues 156-160 in particular are critical in mediating the interactions between effector and active sites and in the T to R quaternary transition.

Phosphofructokinase (PFK) catalyzes the formation of fructose 1,6-bisphosphate and ADP from fructose 6-phosphate (Fru6P) and ATP and is the main regulatory enzyme in glycolysis. The enzyme from *Escherichia coli* exhibits Michaelis-Menten kinetics with respect to ATP but cooperative kinetics with respect to Fru6P, the allosteric activator ADP, and the allosteric inhibitor phosphoenolpyruvate (PEP). The kinetics of *E. coli* PFK were thoroughly studied by Blangy et al. (1968) and were the first enzyme kinetics shown to fit to the Monod-Wyman-Changeaux (Monod et al., 1965) model of cooperativity (MWC). Blangy et al. showed that the kinetics fit well to a two-state "K-system" model, in which PFK exists in states with high (R) and low (T) affinity for Fru6P. This model contrasts with a "V-system" model in which the different forms of the enzyme have different k_{cat} values rather than different binding constants. The MWC model is used in this paper as the conceptual framework for understanding wild-type and mutant PFKs, although the truth is undoubtedly

† C.E.K. is a Fellow of the Jane Coffin Childs Memorial Fund for Medical Research, and this work was supported in part by the Jane Coffin Childs Memorial Fund for Medical Research.
‡ Medical Research Council.
§ University of Colorado.

0006-2960/91/0430-1478$02.50/0

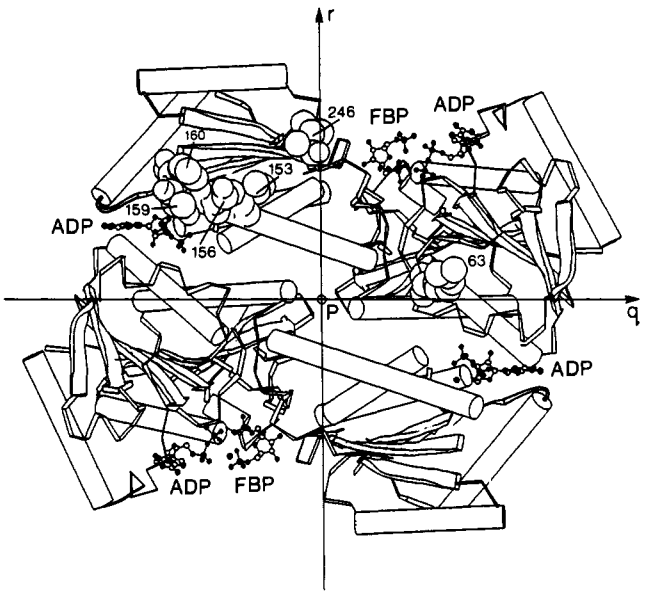

FIGURE 1: Locations of mutations in the PFK structure. The α-carbon trace of two subunits of the *E. coli* R-state tetramer are shown with α-helices depicted as cylinders and β-sheet strands as arrows. Fructose 1,6-bisphosphate (FBP), ADP (indicating the active site products), and ADP (indicating the effector site) are shown with a ball and stick representation. The side chains of all mutated residues are shown with a CPK representation in one subunit. The three 2-fold symmetry axes (*p*,*q*,*r*) relate the subunits of the tetramer to one another. If the *q* and *r* axes are regarded as in the plane of the paper, then the depicted subunits lie behind the plane of the paper, and the other two subunits are generated by rotating the depicted subunits 180° about the *q* or *r* axis to place a pair of subunits above the paper. The subunit interface lying in the plane of the paper is the homotropic interface. The quaternary structure change R to T is a clockwise 7° rotation about the *p* axis of the pair of subunits above the plane of the paper.

more complex than the simple two-state model.

When this work was begun, the crystallographic structures of several forms of PFK had been determined, of both *E. coli* PFK and the homologous enzyme from *Bacillus stearothermophilus* (55% identical in sequence): (1) PFK complexed with Fru6P and presumed to be R-state (2.4-Å resolution) (Evans & Hudson, 1979; Evans et al., 1981); (2) *B. stearothermophilus* PFK complexed with a PEP analogue and presumed to be T-state (7.0 Å) (Evans et al., 1986); (3) *E. coli* PFK complexed with reaction products and presumed to be R-state (2.4 Å) (Shirakihara & Evans, 1988); (4) unliganded *E. coli* PFK (2.4 Å) (Rypniewski & Evans, 1989). The unliganded structure exhibits the same quaternary structure as the R-state. The R- and T-states differ primarily in their quaternary structure: one pair of subunits is rotated 7° with respect to the other pair (Figure 1) (Evans et al., 1986). Although the R-state structure had been crystallized in three different ligation states, efforts to produce crystals of the T-state diffracting to better than 7-Å resolution had failed at the time this work had begun. During the course of this work, however, improved T-state crystals of the *B. stearothermophilus* PFK were grown, and the structure was refined at 2.5-Å resolution (Schirmer & Evans, 1990). This structure showed that the quaternary structure change was triggered by a conformational change in the 6-F loop (residues 156–162) which also removes an arginine side chain from the active site, so that the T-state cannot bind the substrate Fru6P with high affinity.

In an effort to obtain crystals of *E. coli* PFK in the T-state, six site-directed mutants were made with the intention of obtaining mutants "locked" in the T-state. Such mutants are also of interest because they provide structural and functional information about the unactivated form of PFK. The kinetics of the six mutants were examined as a function of Fru6P, ATP, GDP, and PEP concentration. All mutants exhibit lower activity than wild type. One mutant PFK shows a 10-fold reduced affinity for Fru6P and altered linkage between the active and effector sites. Two other mutants exhibit kinetics consistent with a protein "locked" in the T-state. These six PFK mutants show that the kinetic properties of PFK are sensitive to interactions in the homotropic interface, that the effector binding site is linked to the active site in part by the 6-F loop (histidine 160 in particular), and that residues between positions 156 and 159 are critical in the T–R transition.

Materials and Methods

Materials. Deoxyoligonucleotides were synthesized on an Applied Biosystems 380B DNA synthesizer. Deoxynucleotide triphosphates and dideoxynucleotide triphosphates for extension and sequencing reactions were from Pharmacia. The Klenow fragment of *E. coli* DNA polymerase I, rabbit muscle aldolase, rabbit muscle glycerol-3-phosphate dehydrogenase/triosephosphate isomerase, rabbit muscle creatine kinase, creatine phosphate, ATP for kinetic assays, GDP, Fru6P, phosphoenolpyruvate, and NADH were obtained from Boehringer Mannheim. The Matrex Blue-A gel was obtained from Amicon. [α-^{32}P]dATP and [α-^{35}S]dATPαS were obtained from Amersham.

Mutant Design. The six mutations made were based on analysis of the PFK structures and sequences available. Sequences available were from *E. coli* (Hellinga & Evans, 1985; Shirakihara & Evans, 1988), *B. stearothermophilus* (Kolb et al., 1980; French & Chang, 1987), and rabbit skeletal muscle (Poorman et al., 1984). The mammalian gene appears to have arisen by gene duplication of an ancestral gene; each half is homologous to the entire prokaryotic PFK gene. The amino acids naturally occurring in each mutated position are listed in Table I for each sequence. The crystallographic structures available were *B. stearothermophilus* R-state at 2.4-Å resolution (Evans & Hudson, 1979; Evans et al., 1981), *E. coli* R-state at 2.4 Å (Shirakihara & Evans, 1988), *E. coli* unliganded R-state at 2.4 Å (Rypniewski & Evans, 1989), and *B. stearothermophilus* T-state based on a molecular replacement model using data to 7.0 Å (Evans et al., 1986). These structures are available from the Protein Data Bank (Brookhaven, NY). The T-state model was obtained at low resolution by rigid-body refinement from the R-state structure, dividing each subunit into eight rigid units (Evans et al., 1986). Thus, although it provided an approximate picture of the relative orientation of subdomain size segments, it did not contain meaningful information at the level of atomic interactions or side-chain conformations.

The rationale behind the mutants was as follows. All references to the structures are to the *B. stearothermophilus* structures, but similar interactions are present in the corresponding *E. coli* R-state. Helix-6, residues 138–161 in the R-state, is closer to the neighboring subunit in the T-state, suggesting that this part of the homotropic interface is more closely packed in the T-state. Residue Leu 153 was mutated to Val in order to create a packing defect that would be preferentially raise the free energy of the R-state (Richards, 1974; Rashin et al., 1986). For the same reason residue Thr 156 was mutated to Gly. Similarly, His 160 was replaced with an Asn in order to preserve the presence of hydrogen-bond donor and acceptor groups on a shorter side chain. The opposite steric strategy was employed for residue Ser 159. This residue is packed closely against the neighboring subunit in the R-state, but the change in quaternary structure in the

T-state model suggested that a larger side chain could be accommodated. Ser 159 was mutated to Asn. Different strategies were used in designing the other two mutants. Residue Val 246 is close to residue 246 related by the *r* symmetry axis in the neighboring subunit (Figure 1). This residue was changed to Thr so that the symmetry-related residues might hydrogen bond across the T-state interface but not in the more widely separated R-state. Similarly, two Arg residues at position 63 and related by the *q* symmetry axis are 4.1 Å apart in the R-state but 3.2 Å apart in the T-state model. Position 63 was mutated to Ser to test the idea that charge repulsion between these Arg residues destabilizes the T-state.

Mutagenesis. The pEMBL8(+)-based vector pHL1 (Lau et al., 1987) contains the *pfkA* insert and was used for site-directed mutagenesis and overexpression of mutant protein. The deoxyoligonucleotides used for site-directed mutagenesis were purified with Millipore C_{18} Sep-Pak cartridges (Waters Associates, Milford, MA). Single-stranded plasmid DNA for mutagenesis and sequencing was prepared with the R408 "helper" phage (Russell et al., 1986). Site-directed mutagenesis was done with the single-primer method (Carter et al., 1985) and the oligonucleotides listed in Table I. Heteroduplexes were transformed into *E. coli* HB101 [Tn:F^+] cells (Hanahan, 1983). Colonies were grown on 2× TYE (16 g of tryptone, 10 g of yeast extract, and 5 g of NaCl per 1 L of medium) plates containing 50 μg/mL kanamycin and 100 μg/mL ampicillin. The colony hybridization screen using the radioactively labeled mutagenic oligonucleotide (Grunstein & Hogness, 1975; Zoller & Smith, 1983) was based on the method of Carter et al. (1985) with the following modifications: (a) the filters were treated with 10% sodium dodecyl sulfate (SDS) for 5 min immediately prior to exposure to 0.5 M NaOH and 1.5 M NaCl, (b) the filters were rinsed in 2× SSC (17.5 g of NaCl and 8.8 g of sodium citrate in 1 L, pH 7.0) after exposure to 1.0 M Tris, pH 7.5, and 1.5 M NaCl, and (c) the filters were soaked in 2× SSC + 0.1% SDS + 100 μg/mL proteinase K for 60 min at 37 °C before being washed in the prehybridization buffer.

An additional step was introduced before sequencing potential mutant colonies to ensure that the colonies being sequenced consisted of homogeneous plasmid populations. Virions containing single-stranded pHL1-derived DNA in place of R408 DNA were prepared from individual candidate mutant colonies. HB101 [Tn:F^+] cells were transduced with the resultant virions and then plated on 2× TYE + 50 μg/mL kanamycin + 100 μg/mL ampicillin. Several resulting colonies (subclones) were individually sequenced by the dideoxy method (Sanger et al., 1977; Bankier & Barrell, 1983). Less than 100% of the subclones were usually mutant, indicating that the parent colony contained wild-type and mutant plasmid. The mutations were verified by sequencing the entire gene with the M13 universal primer and intragenic primers (Hellinga & Evans, 1985).

Protein. Mutagenized pHL1 vector was transformed (Hanahan, 1983) or transduced (using the virions described in the preceding paragraph) into an *E. coli* strain with both PFK genes deleted: DF1020 [*pro*-82, Δ*pfkB*201, *recA*56, *enda*1, Δ(*rha-pfka*)200, *hsdR*17, *supE*44]. Single colonies were picked and grown overnight in 10 mL of 2× TYE + 100 μg/mL ampicillin; 10 mL of overnight culture was used to inoculate 1 L of 2× TYE containing 100 μg/mL ampicillin and 70 μg/mL isopropyl β-D-thiogalactoside. Cells were grown for approximately 24 h at 37 °C.

Cells were harvested by centrifugation for 20 min at 3000 rpm at 4 °C. Pelleted cells were resuspended in 15 mL of low-salt buffer: 50 mM Tris, pH 7.9, 1 mM ethylenediaminetetraacetic acid (EDTA), and 10 mM dithiothreitol (DTT). Resuspended cells were stored in 2-mL aliquots at 20 °C after being frozen with liquid nitrogen.

Two-milliliter aliquots of resuspended cells were thawed in a 45 °C water bath; 20 μL of 100 mM phenylmethanesulfonyl fluoride (PMSF) was added to the cells, and the cells were sonicated at 4 °C. Another 20 μL of 100 mM PMSF was added to the suspension before centrifugation at 40000 rpm for 90 min with a Beckman 75Ti rotor. The cleared supernatant was loaded onto a 1-mL column of Amicon Matrex Blue-A previously equilibrated with low-salt buffer, and the following were applied in order: (1) 1 mL of low-salt buffer, (2) 4 mL of low-salt buffer plus 1.5 M NaCl, and (3) 5 mL of low-salt buffer plus 2 mM ATP and 10 mM $MgCl_2$. PFK eluted in the presence of the ATP/Mg^{2+}. The column was cleaned for subsequent use with 3 mL of 8 M urea + 0.5 M NaOH followed by 5 mL of low-salt buffer containing 0.02% sodium azide. PFKs were stored as a 50% glycerol solution at −20 °C.

Glycerol and ATP were removed by gel filtration on a 23-mL Sephacryl S-200 column equilibrated with 10 mM Tris, pH 7.9, 0.2 mM EDTA, and 2 mM DTT. Fractions containing PFK were concentrated on a Amicon Centricon-30 filtration unit at 4000 rpm and 4 °C. Protein concentration was determined by measuring the absorbance at 278 nm and using $\epsilon_{278} = 0.6$ cm^2 mg^{-1} (Kotlarz & Buc, 1977). Purified protein was stored at 4 °C after addition of 1 M DTT to a final concentration of 10 mM. RS63 stored at 4 °C did not exhibit a constant reaction velocity in the assay conducted at 25 °C. Rather, the reaction velocity increased with time. This acceleration was proportional to the square of the enzyme concentration (data not shown) and may have been due to the mutant enzyme dissociating into dimers at 4 °C. To prevent this acceleration, RS63 was incubated at 25–37 °C overnight prior to kinetic measurements. All other PFKs were stored at 4 °C until assayed. The purification procedure consistently yielded over 100 mg of PFK/L of culture and produced a single band on polyacrylamide–sodium dodecyl sulfate gels stained with Coomassie Blue.

The PFK activity was measured at 25 °C with a coupled enzyme assay that couples the production of fructose 1,6-bisphosphate to the oxidation of NADH, which is followed spectrophotometrically (Kotlarz & Buc, 1982). The reaction mixture, with a final volume of 1 mL, contained ~34 μg of aldolase, ~17 μg of triosephosphate isomerase, ~2 μg of glycerol-3-phosphate dehydrogenase, 100 mM Tris-HCl, pH 8.0, 10 mM $MgCl_2$, 10 mM NH_4Cl, and 0.2 mM NADH; 10 μg of creatine kinase and 1 mM creatine kinase were also included to maintain constant levels of ATP during the assay. Required amounts of Fru6P, ATP, GDP, and PEP were added from stock solutions, typically 2–10 μL of a 100 mM solution. GDP was used as the activator rather than the physiological ADP because both are comparably active as activators but ADP is a significant competitive inhibitor of the ATP binding site (Blangy et al., 1968). ATP was added last to initiate the reactions. A ΔA_{340}/min = 1 corresponds to 12.4 units of PFK activity. Reaction rates were determined with the linear regression routine of the DU Data Leader program (Beckman Instruments, Fullerton, CA), and the kinetic models were fitted to the rates with the program ENZFITTER (Leatherbarrow, 1987).

Results

Mutant PFKs. Six mutant PFKs were produced (Table I). The mutation designed as TG156 was isolated as T(GS)156;

Table I: Mutant Sequences

position	EC	Bs	RM-N	RM-C	oligonucleotide[b]	mutation[c]
63	R	R	L	Q	TACCGCCACTGTTGATCAT	RS63
153	L	I	I	I	TGTCACGCACACGGTCGAT	LV153
156	T	T	T	S	GAAGAAGAGCCGTCACGCAG	T(GS)156
159	S	S	S	G	CGCTGGTGATTAGAAGAGGT	SN159
160	H	H	H	T	TACGCTGGTTAGAAGAAGAG	HN160
246	V	V	V	V	GGCCCAGCGTAGTTGCGCG	VT246

[a] Ec = *E. coli*, Bs = *B. stearothermophilus*, RM-N = N-terminal half of rabbit muscle, and RM-C = C-terminal half of rabbit muscle. [b] The deoxyoligonucleotides are written in the 5′ to 3′ direction. [c] The notation RS63 denotes the mutant protein which contains a serine residue rather than the wild-type arginine at position 63. The notation T(GS)156 denotes the mutant which contains a glycine rather than the wild-type threonine residue at position 156 and also contains an inserted serine residue.

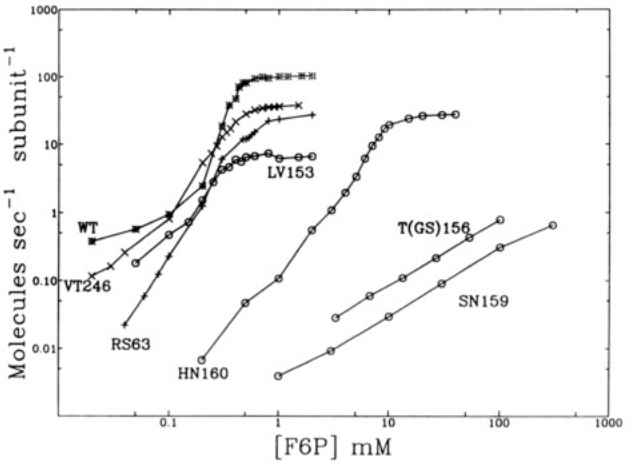

FIGURE 2: Activity versus Fru6P concentration. Sigmoidal kinetic curves remain sigmoidal in a log–log plot (wild type, RS63, LV153, VT246, HN160).

i.e., it contained a Ser insert as well as the Thr to Gly mutation. The wild-type gene (Hellinga & Evans, 1985) contains three TCT serine codons coding for serines 157, 158, and 159 in the protein. It appears that the mutagenic oligonucleotide for TG156 hybridized to the single-stranded template DNA such that one serine codon was "looped out" of the heteroduplex and gave rise to an additional serine codon in the mutant DNA strand. Two colonies out of about 100 hybridized particularly strongly with the radioactively labeled oligonucleotide; sequencing showed that both colonies contained the serine insert.

Activity as a Function of Fructose 6-Phosphate (Fru6P). Four mutants exhibited cooperativity with respect to Fru6P. Three mutants (VT246, RS63, and LV153) show decreased activity compared to wild type but are still cooperative with respect to Fru6P (Figure 2; Table II). One mutant, HN160, has a 10-fold higher $S_{1/2}$ than wild type but retains full cooperativity (Figure 2; Table II).

The two remaining mutants are not cooperative with respect to Fru6P (Figure 2). The kinetic response of SN159 is linear below about 100 mM and increases slower than concentration for higher values of Fru6P. The simplest interpretation of this behavior is that SN159 is a Michaelis–Menten-type enzyme, i.e., noncooperative, which exhibits hyperbolic kinetics with respect to Fru6P with an $S_{1/2} \gtrsim 450$ mM (Table II). Since the SN159 kinetics were not saturated even at 300 mM Fru6P, the $S_{1/2}$ and n_h values are approximate. The T(GS)156 mutant kinetics shows a linear response to Fru6P concentration up to 100 mM. k_{cat}, $S_{1/2}$, and n_h cannot be estimated from linear kinetics. If T(GS)156 is a Michaelis–Menten-type enzyme, then this region of the kinetics curve is the linear region of the hyperbolic curve where the Fru6P concentration is far below $S_{1/2}$. This mutant then would appear to have an $S_{1/2}$ well above 100 mM Fru6P.

Activity as a Function of ATP. The activity of wild-type

Table II: Fru6P Kinetics[a]

enzyme	k_{cat} (mol s^{-1} subunit^{-1})	$S_{1/2}$ (mm Fru6P)	n_h
wild type	120 (14)	0.4	4.0
VT246	34.8 (4.1)	0.38 (0.01)	3.2 (0.1)
RS63	26.6 (1.4)	0.55 (0.11)	3.4 (0.4)
LV153	5.3 (1.6)	0.28 (0.01)	2.7 (0.3)
HN160	27.5 (0.8)	7.4 (0.7)	4.0 (0.1)
T(GS)156	>1	>50	nd
SN159	>1.9[b]	>400[b]	1[b]

[a] All values for mutant proteins are the result of two to four determinations. The standard deviation is given in parentheses. [b] Assuming SN159 is a Michaelis–Menten enzyme.

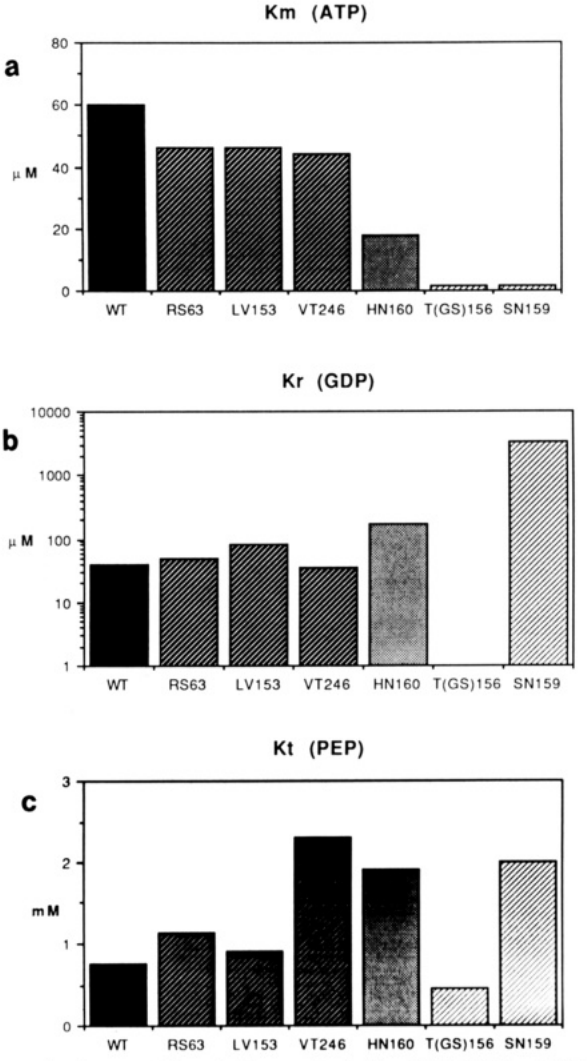

FIGURE 3: Apparent dissociation constants for ATP, GDP, and PEP.

PFK and the six mutant PFKs shows a hyperbolic dependence on ATP concentration; the K_m values are shown in Figure 3a. The determinations were made at saturating concentrations

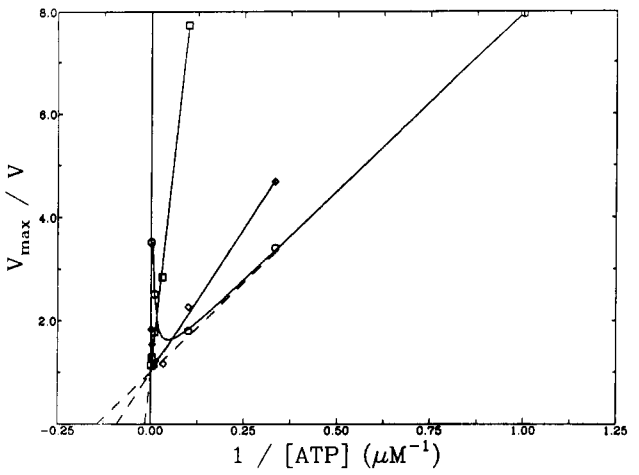

FIGURE 4: Dependence of K_M(ATP) on Fru6P concentration for wild-type PFK: 1 mM Fru6P (square), 0.3 mM Fru6P (diamond), and 0.2 mM Fru6P (circle). The curved line shows that at low concentrations of Fru6P the enzyme is inhibited by high ATP concentrations.

of Fru6P for all PFKs except T(GS)156 and SN159, which could not be saturated. The values for these mutants obtained under nonsaturating conditions (10 mM Fru6P) are comparable to the value obtained for wild-type PFK at 5% Fru6P saturation (Figure 4). The wild-type K_m is higher than that for any mutant.

Activity as a Function of GDP and PEP. The concerted transition theory of Monod et al. (1965) describes the kinetic properties of wild-type PFK quantitatively and was used to obtain apparent dissociation constants for GDP to the R-state [K_r(GDP)] and PEP to the T-state [K_T(PEP)] for those mutants exhibiting cooperative kinetics with respect to effector (Blangy et al., 1968; Lau et al., 1987).

The K_R(GDP) values obtained for mutants RS63, LV153, VT246, and HN160 are within a factor of 2 of that of wild type (Figure 3b). RS63, LV153, and VT246 show a cooperative response to GDP concentrations. HN160 and SN159, however, show a hyperbolic response to GDP. SN159 has a K_R 100-fold higher than wild type and is activated only 2-fold at 10 mM Fru6P. The T(GS)156 mutant is insensitive to GDP concentration up to 3.3 mM.

The K_T(PEP) values of mutants RS63, LV153, and VT246 are also within a factor of 3 of that of wild type (Figure 3c) and show a cooperative response to PEP. Mutants HN160, SN159, and T(GS)156 have dissociation constants similar to that of wild type, but these mutants exhibit a hyperbolic response to PEP. HN160 can be completely inhibited by PEP at 10 mM Fru6P whereas SN159 is inhibited only about 25% at saturating concentrations of PEP and 10 mM Fru6P. The T(GS)156 mutant is activated, rather than inhibited, by PEP: at 1 mM Fru6P, saturating levels of PEP activate T(GS)156 by about 10-fold.

Discussion

The chief aim of this work was to produce PFK mutants which are "locked" in the inactive quaternary structure. Such mutants would be expected to have the following kinetic properties: (a) hyperbolic dependence on both Fru6P and ATP (wild-type PFK has a sigmoidal dependence on Fru6P and a hyperbolic dependence on ATP), (b) $S_{1/2}$(Fru6P) (the Fru6P concentration at which the reaction proceeds at 50% V_{max}) much greater than the 0.4 mM of wild type, and (c) hyperbolic dependence, if any, on the activator GDP and the inhibitor PEP. A hyperbolic activation or inhibition would arise from a modulation of activity within one conformational state, with no communication between effector sites on different subunits. The MWC model predicts that a locked mutant would be insensitive to effectors.

The mutant PFKs can be grouped into three classes on the basis of their kinetic properties: (1) similar to wild type, (2) low Fru6P affinity, and (3) putative T-state. The first group is composed of RS63, LV153, and VT246. These residues are 10–18 Å from the nearest substrate atom and are located in the homotropic interface (Figure 1). Despite the large distance from the active site, all three mutants have a k_{cat} lower than that of wild-type PFK. These mutants are still cooperative with respect to Fru6P, GDP, and PEP and have values of $S_{1/2}$, K_R(GDP), and K_T(PEP) similar to those of wild type. The K_m for ATP is slightly lower for these mutants than for wild type. The lower value of K_m is due in part to the reduction of k_{cat} (since K_m is not a true binding constant) and perturbations in Fru6P binding (see below). To a first approximation, then, these three mutants have kinetic properties similar to those of wild type except for reduced activity.

These mutants demonstrate that mutations in the homotropic interface 10–18 Å from the active site can affect the enzyme's kinetics. The Arg 63 side chain makes interactions with Asp 155 and Asp 59 on neighboring subunits in the R-state. Disruption of this system of salt bridges and/or hydrogen bonds by mutating Arg 63 to Ser decreases the cooperativity of the T–R transition only slightly but is not sufficient to lock PFK in the T-state. The change in electrostatic charge created by this mutant suggests that the interactions at this site do not act as a switch for the T–R transition. The deletion of one methyl group in the LV153 mutant is a more conservative mutation and apparently PFK can tolerate the presence of a cavity or can readily adopt structural changes to fill the cavity at this site in the homotropic interface. The VT246 mutation is also modest, changing a methyl group to a hydroxyl. The possibility of making an additional hydrogen bond across the homotropic interface is not enough to have a major effect on the kinetic properties of PFK. The lack of major changes in the kinetic properties of these mutants indicates that either these sites are not critical for the regulation of the T–R transition or these mutations are conservative with respect to function.

The HN160 mutant is the sole member of the second class. In the R-state of the protein, the histidine side chain constitutes part of the well-packed active site and is in the second hydrogen-bonding shell around substrate (Shirakihara & Evans, 1988). In a recent model of the *B. stearothermophilus* T-state (Schirmer & Evans, 1990), the histidine is 5 Å away from its R-state conformation, is 4.5 Å away from the active site, and is exposed to solvent. Because the T-state conformation of residue 160 is highly exposed to solvent, the mutant's kinetic properties are most simply explained in terms of differences in the R-state conformation. Thus, the 10-fold increase in $S_{1/2}$ observed for HN160 is probably due to disruptions in the Fru6P binding site in the R-state. Model binding suggests that this mutation will disrupt the well-packed native structure and perturb the conformation of residues thought to be important for mediating allosteric effects [e.g., Arg 72 (Berger & Evans, 1990)]. The reduced binding affinity for Fru6P also leads to a reduced K_m for ATP since Fru6P and ATP binding is antagonistic; K_m(ATP) decreases as Fru6P becomes nonsaturating for wild type (Figure 4).

The increases in K_R(GDP) and K_T(PEP) are not the result of direct interactions with the effector; His 160 is over 10 Å from the effector binding site. His 160 is, however, part of the 6-F loop (residues 156–162) which lies between the effector

and active sites and changes conformation in the R–T transition (Schirmer & Evans, 1990). The mutation may lead indirectly to a disruption of the effector site in the R-state, leading to a high value of K_R(GDP). Since the side chain is exposed to solvent in the T-state, the elevated K_T(PEP) is perhaps most likely due to an increase in PEP binding to the disrupted R-state effector site (Lau et al., 1987). In short, the kinetic properties of HN160 can be most simply explained in terms of a direct perturbation of the R-state Fru6P binding site and a perturbation transmitted to the R-state effector binding site.

The last class of mutants, T(GS)156 and SN159, have kinetics with respect to substrate consistent with an enzyme "locked" in one quaternary structure with noncooperative interaction between active and effector sites. These mutations are also in the 6-F loop, between, but not part of, the effector and active sites. The simplest interpretation of these mutants is that they are Michaelis–Menten-type enzymes with respect to Fru6P and ATP. The $S_{1/2}$(Fru6P) for both mutants exceeds 100 mM, orders of magnitude above the 12 μM dissociation constant for the R-state (Blangy et al., 1968). The K_m(ATP) reported for these mutants are lower than the wild-type value because ATP and Fru6P binding are antagonistic (Figure 4) and the K_m(ATP) was determined in nonsaturating Fru6P.

Although the Fru6P kinetics are not cooperative, a linkage appears to remain between the effector and active sites since GDP modulates SN159 kinetics and PEP modulates both T(GS)156 and SN169 kinetics in a hyperbolic manner. This contrasts with the predictions of the MWC model that GDP and PEP would have no effect on the kinetics of a locked T-state mutant. The observation that wild-type PFK fully saturated by Fru6P undergoes an additional 25% increase in activity upon the addition of saturating GDP (data not shown) shows that effector binding to the R-state can also modulate activity. Thus, the simplest MWC model for PFK is inadequate and must be revised to allow effector binding to modulate the activity without a change of quaternary structure.

There is a precedent for the PEP activation seen in T(GS)156; the mutation EA187 (n_h = 3.7; $S_{1/2}$ = 0.75 mM Fru6P) is activated 7-fold at 0.3 mM Fru6P (Lau & Fersht, 1987). Residue 187 is part of the effector binding site which is not between the effector and the active site. Since the T(GS)156 mutant affects residues which are in between the effector and active sites, but not part of either, it appears that there is more than one way to alter the linkage between sites such that PEP becomes an activator.

The reason for the T-state properties of SN159 seems clear. The larger Asn residue in the SN159 mutant cannot be accommodated in the R-state without severe steric clashes, while in the T-state (Schirmer & Evans, 1990) residue 159 extends into the solvent, allowing space for an Asn at residue 159. In contrast, the insertion of a Ser in the T(GS)156 mutant is adjacent to a run of three Ser residues in the wild-type PFK, and it is hard to predict the possible structural perturbations. The insertion would rotate the C-terminus of helix-6 by 100°, translating the helix terminus by 1.5 Å and possibly altering the conformation of the loop linking helix-6 to strand F. The large extent of these possible structural perturbations prevents a detailed molecular interpretation of T(GS)156 from being made without the crystal structure of the mutant.

Comparison of the R- and T-state structures of *B. stearothermophilus* PFK (Schirmer & Evans, 1990) shows that conformational change in the 6-F loop (residues 156–162) is critical in triggering the quaternary structure change, thus linking together the four active sites in the tetramer. The importance of this loop is confirmed by the large perturbations in the allosteric behavior of the mutants in residues 156, 159, and 160. Although an oversimplification, the pattern of a quaternary structure change linked to a conformational change in a short region of polypeptide chain in the subunit interface seems to be common to all the allosteric proteins whose structures are known in both active and inactive conformations, i.e., hemoglobin (Baldwin & Chothia, 1979), aspartate transcarbamylase (Kantrowitz & Lipscomb, 1988), and glycogen phosphorylase (Barford & Johnson, 1989).

The SN159 mutant seems to be a good model of the T-state conformation, in that its kinetic properties are as expected of the T-state. This needs to be confirmed (a) by determining the crystal structure of SN159 and comparison with the *B. stearothermophilus* T-state structure and (b) by determining the actual binding constants of the ligands to PFK (e.g., using equilibrium dialysis or fluorescence). Preliminary equilibrium dialysis results show that SN159 does not bind Fru6P up to 0.5 mM Fru6P (D. Deville-Bonne, personal communication).

Acknowledgments

We thank S. A. Berger, M. Gait, J. Karn, and T. Schirmer for useful discussions.

References

Baldwin, J., & Chothia, C. (1979) *J. Mol. Biol. 129*, 175–220.
Bankier, A. T., & Barrell, B. G. (1983) *Tech. Life Sci. B501*, 2–34.
Barford, D., & Johnson, L. N. (1989) *Nature (London) 340*, 609–616.
Berger, S. A., & Evans, P. R. (1990) *Nature (London) 343*, 575–576.
Blangy, D., Buc, H., & Monod, J. (1968) *J. Mol. Biol. 31*, 13–35.
Carter, P., Bedouelle, H., Waye, M. M. Y., & Winter, G. (1985) *Oligonucleotide Site-Directed Mutagenesis in M13*, Anglian Biotechnology Limited, Colchester, U.K.
Chung, C. T., & Miller, R. H. (1988) *Nucleic Acids Res. 16*, 3580.
Evans, P. R., & Hudson, P. J. (1979) *Nature (London) 279*, 500–504.
Evans, P. R., Farrants, G. W., & Hudson, P. J. (1981) *Philos. Trans. R. Soc. London B293*, 53–62.
Evans, P. R., Farrants, G. W., & Lawrence, M. C. (1986) *J. Mol. Biol. 191*, 713–720.
French, B. A., & Chang, S. H. (1987) *Gene 54*, 65–71.
Grunstein, M., & Hogness, D. S. (1975) *Proc. Natl. Acad. Sci. U.S.A. 72*, 3961–3965.
Hanahan, D. (1983) *J. Mol. Biol. 166*, 557–580.
Hellinga, H. W., & Evans, P. R. (1985) *Eur. J. Biochem. 149*, 363–373.
Kantrowitz, E. R., & Lipscomb, W. N. (1988) *Science 241*, 669–674.
Kolb, P., Hudson, P. J., & Harris, J. L. (1980) *Eur. J. Biochem. 108*, 587–597.
Kotlarz, D., & Buc, H. (1977) *Biochim. Biophys. Acta 484*, 35–48.
Kotlarz, D., & Buc, H. (1982) *Methods Enzymol. 90*, 60–70.
Lau, F. T.-K., & Fersht, A. R. (1987) *Nature (London) 326*, 811–812.
Leatherbarrow, R. J. (1987) *Enzfitter: A Non-Linear Regression Data Analysis Program for the IBM PC*, Elsevier Science Publishers, BV, Amsterdam, The Netherlands.
Monod, J., Wyman, J., & Changeux, J. P. (1965) *J. Mol. Biol. 12*, 88–118.
Poorman, R. A., Randolph, A., Kemp, R. G., & Heinrikson,

R. L. (184) *Nature (London) 309*, 467-469.
Rashin, A., Iofin, M., & Honig, B. (1986) *Biochemistry 25*, 3619-3625.
Richards, F. M. (1974) *J. Mol. Biol. 82*, 1-14.
Russell, M., Kidd, S., & Kelley, M. R. (1986) *Gene 45*, 333-338.
Rypniewski, W. R., & Evans, P. R. (1989) *J. Mol. Biol. 207*, 805-821.
Sanger, F., Nicklen, S., & Coulson, A. R. (1977) *Proc. Natl. Acad. Sci. U.S.A 74*, 5463-5467.
Schirmer, T., & Evans, P. R. (1990) *Nature (London) 343*, 140-145.
Shirakihara, Y., & Evans, P. R. (1988) *J. Mol. Biol. 204*, 973-994.
Zoller, M. J., & Smith, M. (1983) *Methods Enzymol. 100*, 468-500.

Enhancement of the Catalytic Properties of Human Carbonic Anhydrase III by Site-Directed Mutagenesis†

David A. Jewell,‡ Chingkuang Tu,§ Shanthi R. Paranawithana,§ Susan M. Tanhauser,‡ Philip V. LoGrasso,§ Philip J. Laipis,‡ and David N. Silverman*,§

Department of Pharmacology and Therapeutics and Department of Biochemistry and Molecular Biology, University of Florida College of Medicine, Gainesville, Florida 32610

Received August 30, 1990; Revised Manuscript Received November 5, 1990

ABSTRACT: Among the seven known isozymes of carbonic anhydrase in higher vertebrates, isozyme III is the least efficient in catalytic hydration of CO_2 and the least susceptible to inhibition by sulfonamides. We have investigated the role of two basic residues near the active site of human carbonic anhydrase III (HCA III), lysine 64 and arginine 67, to determine whether they can account for some of the unique properties of this isozyme. Site-directed mutagenesis was used to replace these residues with histidine 64 and asparagine 67, the amino acids present at the corresponding positions of HCA II, the most efficient of the carbonic anhydrase isozymes. Catalysis by wild-type HCA III and mutants was determined from the initial velocity of hydration of CO_2 at steady state by stopped-flow spectrophotometry and from the exchange of ^{18}O between CO_2 and water at chemical equilibrium by mass spectrometry. We have shown that histidine 64 functions as a proton shuttle in carbonic anhydrase by substituting histidine for lysine 64 in HCA III. The enhanced CO_2 hydration activity and pH profile of the resulting mutant support this role for histidine 64 in the catalytic mechanism and suggest an approach that may be useful in investigating the mechanistic roles of active-site residues in other isozyme groups. Replacing arginine 67 in HCA III by asparagine enhanced catalysis of CO_2 hydration 3-fold compared with that of wild-type HCA III, and the pH profile of the resulting mutant was consistent with a proton transfer role for lysine 64. Neither replacement enhanced the weak inhibition of HCA III by acetazolamide or the catalytic hydrolysis of 4-nitrophenyl acetate.

Carbonic anhydrase III (CA III)[1] is found almost entirely in skeletal muscle where it can comprise as much as 20% of soluble protein (Shiels et al., 1984). It is the least efficient of the seven isozymes of carbonic anhydrase now known to occur in higher vertebrates (Tashian, 1989). The maximal catalytic turnover number for CA III is near 1×10^4 s^{-1} (Ren et al., 1988; Kararli & Silverman, 1985), 100-fold less than that for human carbonic anhydrase II (1.4×10^6 s^{-1}; Khalifah, 1971), the most efficient of the carbonic anhydrase isozymes found in red cells and secretory tissues (Maren, 1967). Moreover, isozyme III is much less susceptible to inhibition by sulfonamides such as acetazolamide than is isozyme II (Sanyal et al., 1982). Bovine CA III and HCA II have similar amino acid sequences, with 60% of the residues identical, and nearly identical backbone structures (Eriksson, 1988). Superposition of these two structures by computerized fit of main-chain atoms showed a root mean square difference of 0.92 Å, although values in the region of the active site are considerably lower (Eriksson, 1988). The position of lysine 64 and arginine 67 with respect to the active-site zinc and its three histidine ligands in the crystal structure of bovine CA III is shown in Figure 1 (Eriksson, 1988). Lysine 64 extends away from the zinc into solution, and arginine 67 points into the active-site cavity but does not extend directly toward the zinc. The distance from the N-ζ of lysine 64 to the zinc is 12.3 Å, and the distance from the C-ζ of arginine 67 to the zinc is 9.2 Å.

In the pathway for catalysis by isozymes II and III of carbonic anhydrase, the substrate CO_2 reacts with the active site when hydroxide is present as a zinc ligand. The subsequent release of HCO_3^- leaves a water molecule on the metal (eq 1). The enzyme with zinc-bound water must transfer a proton

$$CO_2 + EZnOH^- + H_2O \rightleftharpoons EZnH_2O + HCO_3^- \quad (1)$$

† This work was supported by a grant from the National Institutes of Health (GM 25154).

* Address correspondence to this author at the Department of Pharmacology and Therapeutics, Box J-267 Health Center, University of Florida College of Medicine, Gainesville, FL 32610-0267.
‡ Department of Biochemistry and Molecular Biology.
§ Department of Pharmacology and Therapeutics.

[1] Abbreviations: HCA III, human carbonic anhydrase III; Ches, 2-(*N*-cyclohexylamino)ethanesulfonic acid; Hepes, 4-(2-hydroxyethyl)-1-piperazineethanesulfonic acid; Mes, 2-(*N*-morpholino)ethanesulfonic acid; Mops, 3-(*N*-morpholino)propanesulfonic acid; Taps, 3-[[tris(hydroxymethyl)methyl]amino]propanesulfonic acid.

0006-2960/91/0430-1484$02.50/0